

Critical analysis of the paramagnetic to ferromagnetic phase transition in $\text{Pr}_{0.55}\text{K}_{0.05}\text{Sr}_{0.4}\text{MnO}_3$

R. Thaljaoui^{a,b,c}, M. Pekala^b, J.-F. Fagnard^c, Ph. Vanderbemden^c

(a) Faculty of Physics, Warsaw University of Technology, Koszykowa 75, 00-662 Warsaw, Poland.

(b) Department of Chemistry, University of Warsaw, Al. Zwirki i Wigury 101, 02-089, Poland.

(c) SUPRATECS, Department of Electrical Engineering and Computer Science (B28), University of Liege, Belgium

Abstract

The critical properties of monovalent doped manganite $\text{Pr}_{0.55}\text{K}_{0.05}\text{Sr}_{0.4}\text{MnO}_3$ around the paramagnetic to ferromagnetic phase transition were investigated through various methods: the modified Arrott plots (MAP), the Kouvel-Fisher method and the critical isotherm analysis. Data obtained near T_c were examined in the framework of the mean field theory, the 3D-Heisenberg model, the 3D-Ising model, and tricritical mean field. The deduced critical exponents values obtained using MAP method were found to be $\beta = 0.44(4)$ with $T_c \approx 303$ K and $\gamma = 1.04(1)$ with $T_c \approx 302$ K. Kouvel-Fisher method supplies the critical values to be $\beta = 0.41(2)$ with $T_c \approx 302$ K and $\gamma = 1.09(1)$ with $T_c \approx 302$ K. The obtained critical parameters show a tendency towards the mean-field behavior, suggesting the existence of long-range ferromagnetic order in the compound studied. The exponent δ deduced separately from isotherm analysis at $T = 303$ K was found to obey to the Widom scaling relation $\delta = 1 + \gamma/\beta$. The reliability of obtained exponents was confirmed by using the universal scaling hypothesis. The itinerant character of ferromagnetism in the present system was also tested by using Rhodes-Wohlfarth's criterion.

Introduction

Perovskite manganites have been extensively investigated because of their rich phase diagrams, the coexistence of both paramagnetic-ferromagnetic and insulator-metal transition and the discovery of the colossal magnetoresistance (CMR) in those materials [1, 2]. The interplay between the magnetic and transport properties has been explained by various theories as the AFM super exchange $\text{Mn}^{3+}-\text{Mn}^{3+}/\text{Mn}^{4+}-\text{Mn}^{4+}$ and the FM double exchange (DE) $\text{Mn}^{3+}-\text{Mn}^{4+}$ interactions, polaronic effects and phase separation [3-5]. The phase transition phenomena are well clarified by the exchange theory and Jahn Teller effect [6]. Recently the exploration of critical phenomena, in particular the determination of critical exponents at the phase transition, has been considered as interesting key for theoretical description and experimental characterization of magnetic materials [7-9]. Previously, the critical behavior in the DE model was described by long-range mean-field theory [10, 11]. However, other reports suggested that the critical behavior should be attributed to short-range Heisenberg model [12, 13]. Therefore, experimental works on critical exponents are still controversial. M. Khelifi et al. [14] reported the 3D-Ising models for $\text{La}_{0.8}\text{Ca}_{0.2}\text{MnO}_3$, it was also reported a 3D Heisenberg universality class for the ferromagnetic manganite $\text{Pr}_{0.6}\text{Sr}_{0.4}\text{MnO}_3$ [9]. Recently, J. Fan [8] reported a simple and efficient method to determine the critical exponent of $\text{Pr}_{0.55}\text{Sr}_{0.45}\text{MnO}_3$ manganite based on the field dependence of magnetic entropy change. Other studies on $\text{Pr}_{0.6}\text{Sr}_{0.4}\text{MnO}_3$ single crystals [9], were based on the independent determination of the three critical exponents..

Recent studies of critical exponent on monovalent (Ag, Li) doped manganites were reported for $\text{La}_{0.5}\text{Ca}_{0.5-x}\text{Ag}_x\text{MnO}_3$ and $\text{La}_{0.5}\text{Ca}_{0.4}\text{Li}_{0.1}\text{MnO}_3$ compounds [15, 16]. Due to the

valence difference, the replacement of the trivalent metals by the monovalent metals converts twice more Mn^{3+} to Mn^{4+} . This weakens the double exchange interaction. The Curie temperature, therefore, is expected to be reduced compared to that reported for the parent undoped manganite $Pr_{0.6}Sr_{0.4}MnO_3$ (310 K). Moreover, it is observed that the 5 % K doping shifts the structural transition to about 150 K, which is about 50 K higher than for the undoped manganite [17, 18]. The aim of the present work is to investigate the critical exponents and the Curie temperature through various techniques including modified Arrott plot, Kouvel-Fisher method, and critical isotherm analysis of potassium doped manganite $Pr_{0.55}K_{0.05}Sr_{0.4}MnO_3$ in order to understand its magnetic interactions. The obtained values were discussed and compared to those reported for similar manganites. According to the Rhodes-Wohlfarth's criterion a itinerant character of ferromagnetism was also tested.

Experimental

$Pr_{0.55}K_{0.05}Sr_{0.4}MnO_3$ samples were prepared by using the standard conventional solid state reaction method at room temperature. Stoichiometric ratio of Pr_6O_{11} , $SrCO_3$, K_2CO_3 and MnO_2 (99.9%) were mixed in an agate mortar and then heated in air to 1000 °C for 60h with intermediate grinding. The obtained mixtures were then pressed into pellets and sintered at 1100 °C in air for 60 h with intermediate grinding. Cell parameters were studied by the X-ray diffraction with Cu-K α radiation (1.54 Å) in the 2 θ range of 10 - 100 degrees. Structural analysis was carried out using the standard Rietveld technique, the average crystallite CXRD size was 70 nm and the volume was 228.334 Å³. The mean grain size value G_{SEM} was estimated from SEM images and was found to be varying between 1 and 1.2 μm. Magnetic measurements were carried out using PPMS (Physical Property Measurement System from Quantum Design) in applied magnetic fields up to 2 T.

AC susceptibility

The temperature dependence of the in-phase AC magnetic susceptibility χ' (T) is shown in Fig. 1. On lowering temperature, the magnetic susceptibility increases rapidly around PM-FM transition temperature T_C , and then decreases in the charge ordered state. Such behavior is in good agreement with that observed for typical ferromagnetic materials. We also note that the T_C value defined by the minimum of $d\chi'(T)/dT$ is found to be equal 303 K (± 1 K), which is in accordance with that determined by the temperature derivative of DC magnetization [17]. According to the sample shape and orientation of the applied magnetic field, the demagnetization factor N can be estimated to be 0.18-0.19 for rectangular ferromagnetic prism [19]. Knowing that the magnetic susceptibility is bounded by 1/N, as can be observed for samples with short aspect ratio [20], it is of interest to compare the measured $\chi'(T)$ temperature dependence with the 1/N demagnetization limit. Since $\chi'(T)$ is substantially smaller than 1/N in most of the investigated temperature range (Fig. 1), we can conclude that demagnetization effects are not predominant in the present case.

Arrott plots

The positive slope of Arrott isotherms for temperatures close to the Curie temperature shown in Fig. 2A, confirms that the studied sample presents a second order phase transition, according to the Banerjee criterion [17, 21]. Generally, the second-order magnetic phase transition behavior is characterized by a set of critical exponents (β , γ and δ) near Curie temperature [10]. This analysis cannot be done for first order transition because the field dependence of the critical temperature [22].

We have prepared the modified Arrott plots (MAP) applying the theoretical exponents for the mean field model, 3D-Heisenberg model, 3D-Ising, and tricritical mean field models. The critical exponents β , γ and δ for each model are listed in table 1 [10, 22]. As shown in Fig. 2A-

D, all MAP in the high field regime ($B > 1$ T, i.e. on the right of the dashed curve) are linear and nearly parallel to each other. We calculated their relative slopes, RS defined as: $RS = S(T)/S(T_c)$, where $S(T)$ and $S(T_c)$ are the slopes deduced from MAP around and at T_c , respectively. Perfect parallel lines are described by RS equal to 1. The results in Fig. 3 indicate that the relative slope (RS) reported for mean field-theory model is the closest to 1, meaning that this model can be suitable for proper choice to deduce the critical exponents.

The critical exponents are defined as follows: [23]

$$M_{sp}(T) = M_0 |t|^\beta, \quad T < T_c, \quad (1)$$

$$\chi_0^{-1}(T) = (H_0/M_0) |t|^\gamma, \quad T > T_c, \quad (2)$$

$$M(H) = RH^{\delta}, \quad (3)$$

where M_{sp} is spontaneous magnetization, χ_0 is the initial magnetic susceptibility, t is the reduced temperature defined as $t = (T - T_c)/T_c$, M_0 , H_0/M_0 and R are the critical amplitudes. For better critical analysis, t was limited to about 0.03. The linear extrapolation from high field regime ($B > 1$ T and the temperature range 272 K to 320 K) to the intercepts with $M^{1/\beta}$ and $(H/M)^{1/\gamma}$ axes was applied to determine the values of $M_{sp}(T)$ for $T < T_c$ and $\chi_0^{-1}(T)$ for $T > T_c$, respectively. The plot of the spontaneous magnetization M_{sp} and the inverse of the initial magnetic susceptibility versus temperature were used to extract the proper values of β , γ and T_c , as shown in Fig. 4. The values deduced from the best fit according to the equation (1) are found to be 0.44(4) for β with $T_c \approx 303$ K and according to the equation (2) are found to be 1.04(1) for γ with $T_c \approx 302$.

The critical exponent δ can be determined from the obtained β and γ values according to the Widom scaling relation [24]:

$$\delta = 1 + \frac{\gamma}{\beta}, \quad (4)$$

and the value was found to be equal 3.34(5). Fig. 5 shows isotherms M (H_{eff} , $T = 300$ K) and M (H_{eff} , $T = 303$ K). According to Eq. (3) and from the linear fit of $\log(M)$ versus $\log(H_{eff})$ plots for high filed range (inset Fig. 5), we deduced $\delta = 3.33(2)$ which fits with $\delta = 3.34(5)$ that deduced from Widom scaling relation Eq. (4). However, the deduced $\delta = 4.16(1)$ from the isotherm at 300 K, is found to be slightly deviated. This result may confirm that the nearest critical temperature can be equal to 303 K.

Kouvel-Fisher method

The critical exponent can be also determined by using the Kouvel-Fisher method, which can provides values that are more accurate because the slope is easy determined without application of log function [25]:

$$\frac{M_{sp}(T)}{dM_{sp}(T)/dT} = \frac{T - T_c}{\beta}, \quad (5)$$

$$\frac{\chi_0^{-1}(T)}{d\chi_0^{-1}(T)/dT} = \frac{T - T_c}{\gamma}, \quad (6)$$

The plots of $M_{sp}(T)[dM_{sp}(T)/dT]^{-1}$ and $\chi_0^{-1}(T)[d\chi_0^{-1}(T)/dT]^{-1}$ shown in Fig. 6 exhibit straight lines. According to the equation (5) and (6), the slopes should be equal to $1/\beta$ and $1/\gamma$, respectively. Then the intercepts correspond to the critical temperature T_c . The deduced values are found to be 0.41(2) for β with $T_c \approx 302$ K and 1.09 (1) for γ with $T_c \approx 302$. According to the Widom scaling relation Eq. (4) the deduced value of δ is found to equal 3.64(2). The

obtained results are comparable with those derived from the modified Arrott plot. This indicates the self-consistency of the values of the exponents.

Scaling theory

For checking the reliability of critical exponents, the scaling theory provides a scope according to the magnetic equation of state in critical region as given [10]:

$$M(H,t) = |t|^\beta f_\pm(H \Big/ |t|^{\beta+\gamma}), \quad (7)$$

where t is the reduced temperature $(T-T_C)/T_C$, f^+ for $T>T_C$ and f^- for $T<T_C$, f^+ and f^- are two regular functions. The plot of $M t^\beta$ versus $H t^{(\beta+\gamma)}$ as shown in Fig. 7 and the log-log scale for the same data in the inset of Fig. 7 show two universal curves for $T > T_C$ and for $T < T_C$, respectively. The existence of these two curves in our case is a good confirmation that our experimental data is in agreement with the scaling theory and consequently the critical exponents are reliable.

In previous studies [17], we reported critical exponent n by using the field dependence of magnetic entropy change thus, we deduced β and γ values which were found to be very similar to those reported in the present work.

The critical exponent n can be also determined by using the following formula [26]:

$$n = 1 + \frac{\beta - 1}{\beta + \gamma} \quad (8)$$

The obtained value is ≈ 0.61 which is in good agreement with 0.59 reported in ref [17] and not so far to the theoretical values 0.66 and 0.63 values reported for the mean field model and the 3D Heisenberg model, respectively. We notice also that the obtained n values equal to 0.61 is very close to the estimated values 0.62 and 0.64 reported for $\text{Pr}_{0.6}\text{Sr}_{0.4}\text{MnO}_3$ and $\text{Pr}_{0.55}\text{Sr}_{0.45}\text{MnO}_3$ manganite [8,9], respectively, as listed in table 1. While the estimated values are found to be deviated to 0.56 and 0.4 values reported for 3D Ising model and tricritical mean field model, respectively.

Discussion

As mentioned above the derived critical exponents are essentially determined from mean field-theory model but the obtained values are not strictly equal to those of mean field-theory model. Such result confirms the complex magnetic behavior of the manganite studied. The β values of 0.41(2) and 0.44(4) deduced from Kouvel-Fisher method and modified Arrott plot, respectively, locate between those expected for the mean-field and 3D Heisenberg models. Consequently, to distinguish the proper model the relative slope plots (RS) was considered. As illustrated in Fig.3 the RS observed for the mean field model results in values closer to the ideal value of 1 more than the remaining three models. This mean field model can be explained by the presence of a long-range FM interactions. The similar behavior was also reported for $\text{Eu}_{0.5}\text{Sr}_{0.5}\text{CoO}_3$ system [27]. A conventional magnetic systems belonging the 3D Heisenberg universality class with short range ferromagnetic (FM) interaction were also reported for undoped $\text{Pr}_{0.6}\text{Sr}_{0.4}\text{MnO}_3$ compound [9, 28]. This means that K - doping favours establishing FM long-range order in $\text{Pr}_{0.6-x}\text{K}_x\text{Sr}_{0.4}\text{MnO}_3$ system. We should also note that the deviation of critical values can be related to other effects as the dimensionality of the magnetic range. The present values were compared to similar doped manganite in table 1.

Generally the long-range type of interaction may occur because of an isotropic interaction between spins, which is generated by the exchange integral range as: [29].

$$J(r) = \frac{1}{r^{d+\sigma}}, \quad (9)$$

where d is the dimension, σ is the range of the interaction and r is the distance. A 3D system of isotropic spins of long-range or short-range type is observed for $\sigma > 2$ or $\sigma < 2$, respectively. The 3D Heisenberg model is valid if $\sigma > 2$, and the exchange integral $J(r)$ decays with distance faster than r^{-5} . However the mean-field model is valid for $\sigma \leq 3/2$, when $J(r) \propto r^{-(3+\sigma)}$ with $3 + \sigma \leq 4.5$. In the intermediate range $3/2 \leq \sigma \leq 2$, the system follows different class depending on σ value. According to [29, 30], for a system with dimensionality d and spin n , the critical exponent γ and the range of interaction σ satisfy a mathematical relation defined as:

$$\gamma = 1 + \frac{4}{d} \left(\frac{n+2}{n+8} \right) \Delta\sigma + \frac{8(n-4)(n+2)}{d^2(n+8)^2} \left[1 + \frac{2G\left(\frac{1}{2}d\right)(7n+20)}{(n-4)(n+8)} \right] \Delta\sigma^2 \quad (10)$$

where $\Delta\sigma = \sigma - \frac{1}{2}d$ and $G\left(\frac{1}{2}d\right) = 3 - \frac{1}{4}\left(\frac{1}{2}d\right)^2$. In the case of the present sample with $\gamma = 1.04(1)$ and by using Eq. (9) one can determine σ value equal to be 1.52(2). This result suggests that $J(r)$ decays as $r^{-4.52}$, which visibly approaches the mean field behavior with long-range interaction.

As mentioned in [26], according to Rhodes-Wohlfarth's criterion [31], in order to determine the nature of the ferromagnetism we calculated the ratio Q_c/Q_s , where Q_s and Q_c are the number of magnetic carriers per atom deduced from low-T saturation magnetization and calculated from effective Curie Weiss constant C , respectively. The value of Q_s is 3.10 at 200 K, and the effective paramagnetic moment μ_{eff}^P calculated from the inverse susceptibility, is found to equal 5.67. Q_c is deduced from the following equation $\mu_{eff}^P = 2g\sqrt{S(S+1)}$, where $S=Q_c/2$ is the effective spin per atom. The deduced value is 4.75 which is higher than the expected value 3.5. This difference can be related to the presence of ferromagnetic clusters above Curie temperature T_c [32]. The deduced values indicate that Q_c/Q_s is larger than 1 which is a confirmation for the itinerant character of ferromagnetism in $\text{Pr}_{0.55}\text{K}_{0.05}\text{Sr}_{0.4}\text{MnO}_3$ compound [30].

Conclusion

Summarizing, critical exponents for $\text{Pr}_{0.55}\text{K}_{0.05}\text{Sr}_{0.4}\text{MnO}_3$ compound have been investigated by using critical isotherm modified Arrott plot and Kouvel–Fisher methods. The deduced critical exponent values were found to be located between the 3D Heisenberg model and the mean-field model. The variation of the relative slope $R_S(T)$ indicates that the mean field model is the most convenient to calculate the critical exponent of $\text{Pr}_{0.55}\text{K}_{0.05}\text{Sr}_{0.4}\text{MnO}_3$ compound. The satisfaction to the scaling theory relation gives confidence on the reliability of the deduced values. The range interaction σ value equal to 1.52(2) suggests that exchange integral $J(r)$ decays as $r^{-4.52}$ which is similar to $r^{-4.5}$ characteristic for the mean field model with long range spin interaction. By using Rhodes-Wohlfarth's criterion, the itinerant character of ferromagnetism in $\text{Pr}_{0.55}\text{K}_{0.05}\text{Sr}_{0.4}\text{MnO}_3$ compound is confirmed.

Acknowledgements. This work was partially supported in the frame of scientific exchange agreement between Belgium (WBI) and Poland.

References

- [1] E. Dagotto, Nanoscale Phase Separation and Colossal Magnetoresistance: The Physics of Manganites and Related Compounds (Springer, Berlin, 2003).
- [2] Y. Tokura, *Rep. Prog. Phys.* 69 (2006) 797.
- [3] C. Zener, *Phys. Rev.* 82 (1951) 403.
- [4] A.J. Millis, P.B. Littlewood, B.I. Shraiman, *Phys. Rev. Lett.* 74 (1995) 5144.
- [5] S. Mori, C.H. Chen, S.W. Cheong, *Phys. Rev. Lett.* 81 (1998) 3972.
- [6] A. J. Millis, *Phys. Rev. B* 53, (1996) 8434.
- [7] J. Fan, L Ling, B Hong, L. Zhang, L. Pi, Y. Zhang, *Phys. Rev. B* 81, (2010) 144426.
- [8] J. Fan, L Pi, L Zhang, W Tong, L Ling, B Hong, Y Shi, W Zhang, D Lu, Y Zhang, *J. Appl. Phys.* 98 (2011) 072508.
- [9] S. Rößler, Harikrishnan S. Nair, U. K. Roessler, C.M.N. Kumar, S Elizabeth, and S. Wirth, *Phys. Rev. B* 84 (2011) 184422.
- [10] H. E. Stanley, *Introduction to Phase Transitions and Critical Phenomena* _Oxford University Press, London, (1971).
- [11] Tran Dang Thanh, Dinh Chi Linh, T. V. Manh, T. A. Ho, The-Long Phan, S. C. Yu, *J. Appl. Phys.* 117, 17C101 (2015)
- [12] Y. Motome, N. Furukawa, *J. Phys. Soc. Jpn.* 69 (2000) 3785
- [13] Y. Motome, N. Furukawa, *J. Phys. Soc. Jpn.* 70 (2001) 1487.
- [14] M. Khelifi, A. Tozri, M. Bejar, E. Dhahri, E.K. Hlil, *J. Magn. Magn. Mater* 13 (2012) 21426.
- [15] M. Smari, I. Walha, A. Omri, J.J. Rousseau, E. Dhahri, E.K. Hlil, *Ceramics International* 40 (2014) 8945
- [16] R. Li, C Zhang, L Pi, Y Zhang, *EPL* 103 (2014) 57010
- [17] R. Thaljaoui, W. Boujelben, M. Pękała, K. Pękała, J. Antonowicz , J.-F. Fagnard, Ph. Vanderbemden, S. Dąbrowska, J. Mucha, *J. Alloys. Compd.* 611 (2014) 427
- [18] R. Thaljaoui W. Boujelben K. M. Pękała M. M. Pękała W. Cheikhrouhou-Koubaa A. Cheikhrouhou *J. Mater. Sci.* 48 (2013) 3894
- [19] A. Aharoni, *J. Appl. Phys.* 83 (1998) 6.
- [20] Ph. Vanderbemden, B. Vertruyen, A. Rulmont, R. Cloots, G. Dhalenne, M. Ausloos *Phys. Rev. B* 68, 224418 (2003)
- [21] S. K. Banerjee, *Phys. Lett.* 12 (1964) 67.
- [22] D. Kim, B. Revaz, B. L. Zink, F. Hellman, J. J. Rhyne, and J. F. Mitchell, *Phys. Rev. Lett.* 89, (2002) 227202.
- [23] M. E. Fisher, *Rep. Prog. Phys.* 30 (1967) 615.
- [24] B. Widom, *J. Chem. Phys.* 43 (1965) 3898; *J. Chem. Phys.* 41 (1964) 1633.
- [25] J. S. Kouvel and M. E. Fisher, *Phys. Rev.* 136 (1964) A1626
- [26] V. Franco, A. Conde, J.M. Romero-Enrique, J.S. Blazquez, *J. Phys.: Condens. Matter.* 20 (2008) 285207.
- [27] Renwen Li, Feng Li, Jun Fang, Wei Tong, Changjin Zhang, Li Pi, Yuheng Zhang, *J. Alloys. Compd* 577 (2013) 303
- [28] Sobhi Hcini, Sadok Zemni, M. Baazaoui, Jamila Dhahri, Henri Vincent, M. Oumezzine, *Solid State Sciences* 14 (2012) 644
- [29] Michael E. Fisher, Shang-keng Ma, B.G. Nickel, *Phys. Rev. Lett.* 29 (1972) 917
- [30] A.K. Pramanik, A. Banerjee, *Phys. Rev. B* 79 (2009) 214426.
- [31] P. Rhodes, E.P. Wohlfarth, *Proc. R. Soc. Lond. A* 273 (1963) 247
- [32] A. K. Pramanik and A. Banerjee, *J. Phys.: Condens. Matter* 20 (2008) 275207

Figures

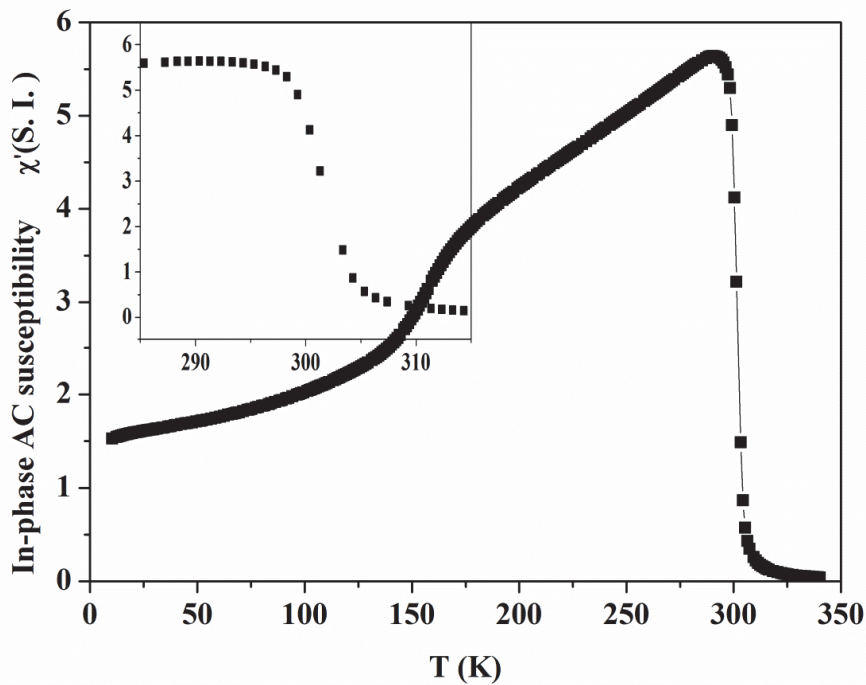


Fig. 1. Temperature dependence of the in-phase AC magnetic susceptibility $\chi'(T)$ under magnetic field of 1 mT for $\text{Pr}_{0.55}\text{K}_{0.05}\text{Sr}_{0.4}\text{MnO}_3$ manganite. Inset shows same plot in temperature range 285 K to 315 K.

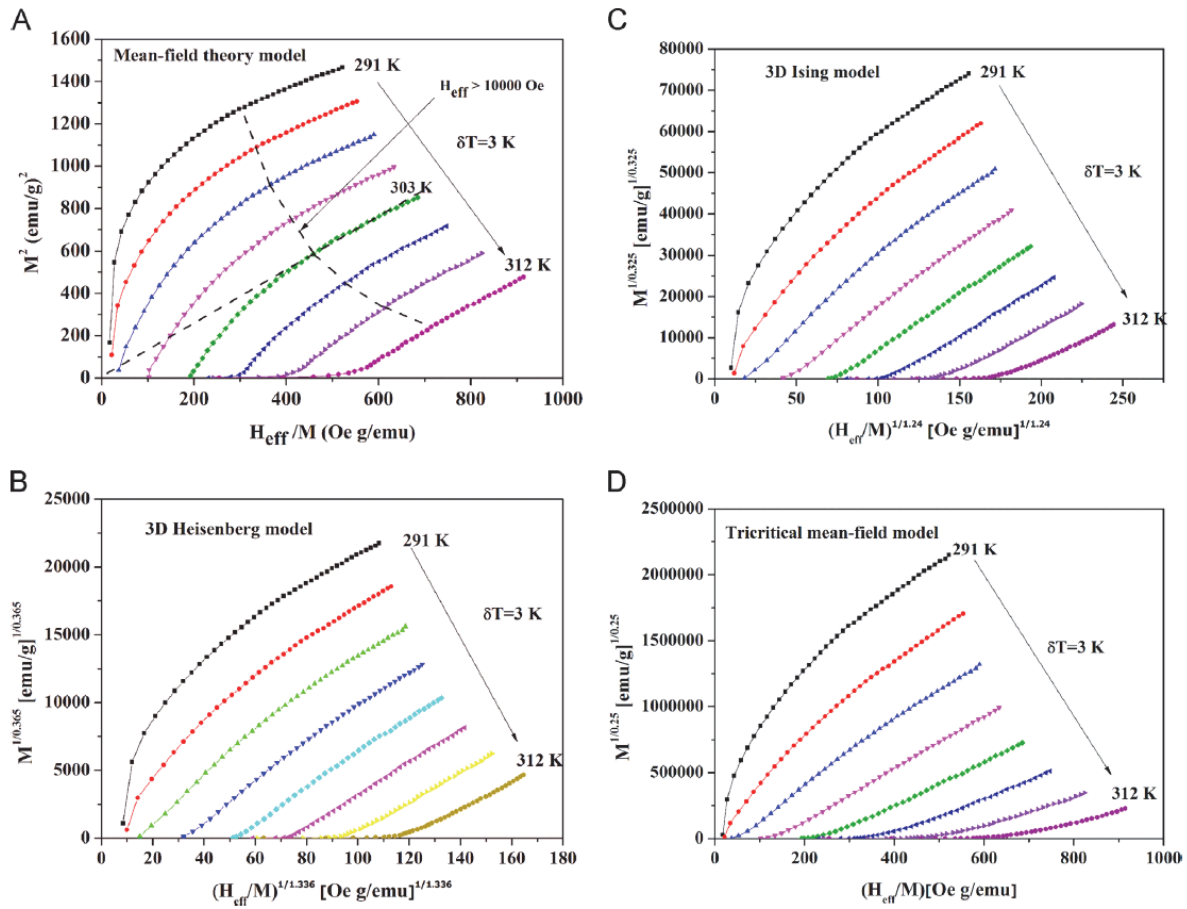


Fig. 2A-D: Modified Arrott plots isotherms: Mean-field model ($\beta = 0.5$; $\gamma = 1$ and $\delta = 3$) (A): the dashed line shows the T_c temperature, the dashed curve indicates the limit of high field regime; 3D–Heisenberg ($\beta = 0.365$; $\gamma = 1.336$ and $\delta = 4.80$) (B), 3D–Ising ($\beta = 0.325$; $\gamma = 1.241$ and $\delta = 4.82$) (C); and tricritical mean field theories ($\beta = 0.25$; $\gamma = 1$ and $\delta = 5$) (D) for $\text{Pr}_{0.55}\text{K}_{0.05}\text{Sr}_{0.4}\text{MnO}_3$ manganite.

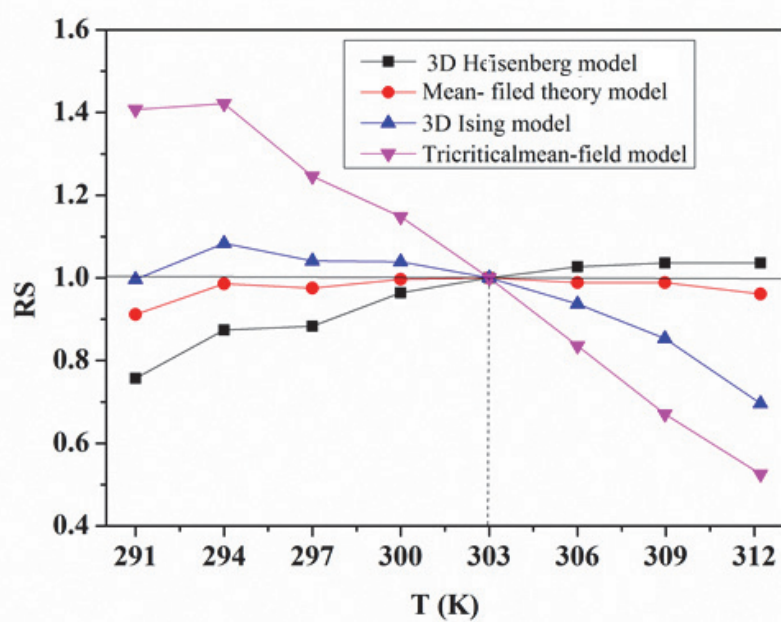


Fig. 3. Relative slope (RS) for $\text{Pr}_{0.55}\text{K}_{0.05}\text{Sr}_{0.4}\text{MnO}_3$ manganite as a function of temperature.

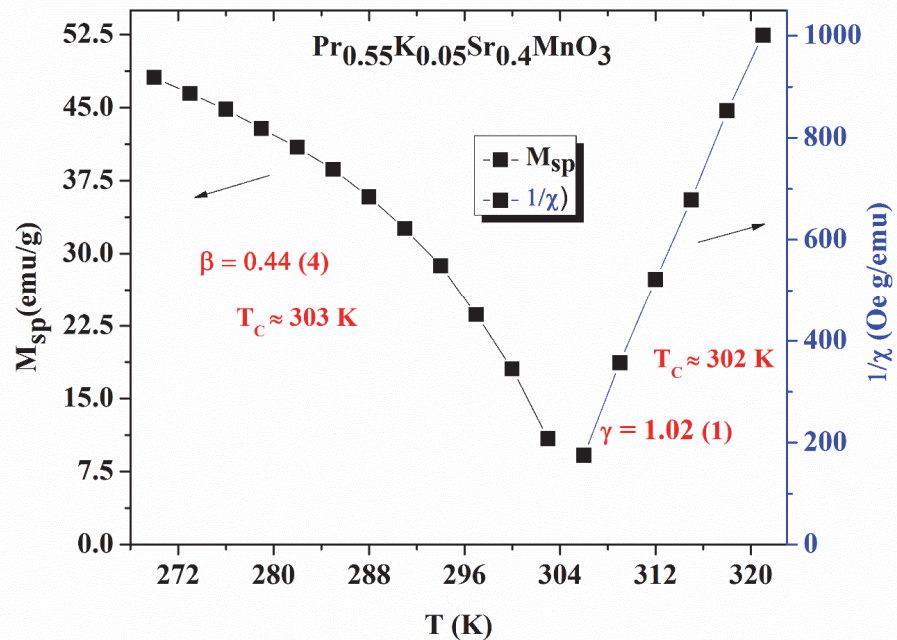


Fig. 4. Spontaneous magnetization M_{sp} and the inverse of the initial magnetic susceptibility versus temperature for $\text{Pr}_{0.55}\text{K}_{0.05}\text{Sr}_{0.4}\text{MnO}_3$ manganite.

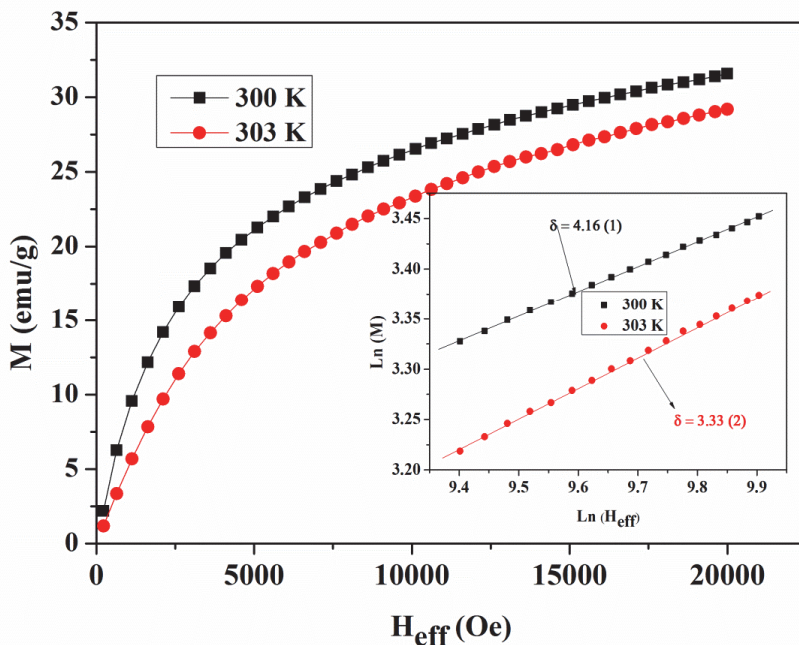


Fig. 5. Isothermal M versus H_{eff} for $\text{Pr}_{0.55}\text{K}_{0.05}\text{Sr}_{0.4}\text{MnO}_3$ manganite at $T = 300$ K and 303 K, Inset show Log-log scale plot of the solid line is the linear fit following eq (3).

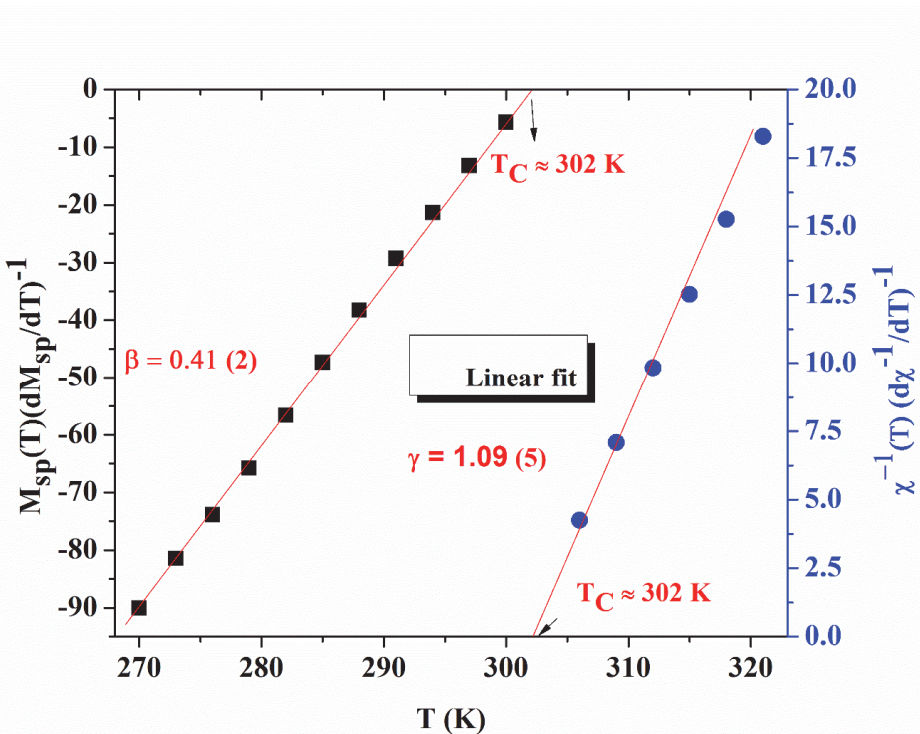


Fig. 6. Kouvel-Fisher plots for the spontaneous magnetization M_{sp} and the inverse of the initial magnetic susceptibility for $\text{Pr}_{0.55}\text{K}_{0.05}\text{Sr}_{0.4}\text{MnO}_3$ manganite.

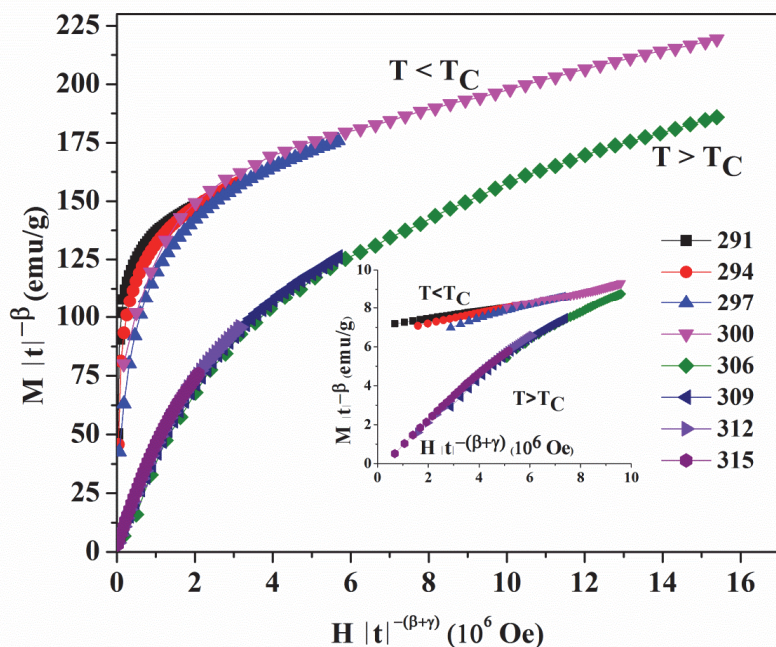


Fig. 7. Scaling plots using β and γ determined by Kovel-Fisher method, the inset is log-log scale for the same plot.

Table 1. Critical parameters β , γ , δ , n and T_c of $\text{Pr}_{0.55}\text{K}_{0.05}\text{Sr}_{0.4}\text{MnO}_3$ compound compared with those of theoretical models and typical manganites. Abbreviation: MF: mean field, MAP: modified Arrott plots; K-F: Kouvel-Fisher method; I-M: Isothermal magnetization.

Composition	Method	T_c (K)	β	γ	n	δ	Reference
$\text{Pr}_{0.6}\text{Sr}_{0.4}\text{MnO}_3$	MAP	301	0.365(4)	1.309(3)	0.62	4.586	[9]
$\text{Pr}_{0.55}\text{K}_{0.05}\text{Sr}_{0.4}\text{MnO}_3$	MF	≈ 303	0.44(4)	1.04(1)	0.61	3.34(5)	This work
	K-F	≈ 302	0.41(2)	1.09 (1)	0.60	3.64(2)	
$\text{Pr}_{0.55}\text{Sr}_{0.45}\text{MnO}_3$	I-M	292	0.449	1.113	0.65	--	[8]
	K-F	290	0.462	1.033	0.64	--	
$\text{Pr}_{0.5}\text{Sr}_{0.5}\text{MnO}_3$	MAP	≈ 261	0.443(6) 0.448(9)	1.339(6) 1.334(1)	0.69	4.022(3) 3.977(6)	[30]
	K-F	≈ 261			0.69		
Mean-field	Theory	--	0.5	1	0.66	3	[10]
3D Heisenberg	Theory	--	0.365	1.386	0.63	4.8	[10]
3D-Ising	Theory	--	0.325	1.24	0.56	4.82	[10]
Tricritical mean field	Theory	--	0.25	1	0.4	5	[22]

$$\delta = 1 + \frac{\gamma}{\beta}, \quad n = 1 + \frac{\beta - 1}{\beta + \gamma}$$